Replication of Mesoporous Aluminosilicate Molecular Sieves (RMMs) with Zeolite Framework from Mesoporous Carbons (CMKs)

Ayyamperumal Sakthivel,[†,||] Shing-Jong Huang,[†] Wen-Hua Chen,[†] Zon-Huang Lan,[†] Kuei-Hsien Chen,[†] Tae-Wan Kim,[‡] Ryong Ryoo,[‡] Anthony S. T. Chiang,[§] and Shang-Bin Liu*[,†]

Institute of Atomic and Molecular Sciences, Academia Sinica, P.O. Box 23-166, Taipei, Taiwan 106, Republic of China, National Creative Research Initiative Center for Functional Nanomaterials, Department of Chemistry, Korea Advanced Institute of Science and Technology, Daejeon 305-701, Republic of Korea, and Department of Chemical and Materials Engineering, National Central University, Chung-Li, Taiwan 320, Republic of China

Received December 9, 2003. Revised Manuscript Received May 26, 2004

A novel class of mesoporous aluminosilicate molecular sieves has been prepared by replication from carbon mesoporous molecular sieves (CMKs) using zeolite precursors and characterized by a variety of analytical and spectroscopic techniques, such as XRD, N_2 adsorption/desorption, SEM/TEM, IR, hyperpolarized (HP) ^{129}Xe, and ^{31}P MAS NMR. These replicated mesoporous materials (RMMs), namely RMM-1 and RMM-3 prepared from CMK-1 and CMK-3, were found to exhibit mesoporous structures respectively analogous to Al-MCM-48 and Al-SBA-15 but possess unique microporous characteristics due to the presence of zeolite secondary building units in the framework. Consequently, these RMMs are also found to have superior thermal, hydrothermal, and mechanical stabilities and with improved acidic properties compared to their respective parent counterparts. The RMM-3 so prepared represents the first synthesis of protonated aluminosilicate with an SBA-15 structure prepared by a nonacidic route.

Introduction

Development of aluminosilicate mesoporous materials with microporous properties is of great interest in the field of catalysts and adsorption.[1] Several approaches have been made in terms of preparing mesoporous molecular sieves with exotic zeolitelike microporous characteristics, for example, by using cotemplating or zeolite seeding synthetic methods.[2−7] Despite much encouraging progress in recent years, the genuine structures, thermal/hydrothermal stability, acidity, and practical applications of these mesoporous/microporous composite materials remain intriguing issues of debate. The fact that most of the aforementioned one-step synthesis methods invoke low pH condition[2−4] makes them difficult to introduce heteroatoms onto the structural framework and hence puts additional constraints in terms of their mass production and commercial applicability. Thus, the development of novel routes to synthesize mesoporous materials with a zeolite secondary building unit remains a demanding task. Jacobsen and co-workers reported the synthesis of zeolite single crystals having uniform size, high BET surface area, and good acidity under the confined space of either carbon black[8] or multiwall carbon nanotube.[9] More recently, novel syntheses of mesoporous ZSM-5 monoliths and zeolite crystals, using carbon aerogel[10] and

* To whom correspondence should be addressed. Fax: +886-2-23620200. E-mail: sbliu@sinica.edu.tw.
† Academia Sinica.
‡ Korea Advanced Institute of Science and Technology.
§ National Central University.
|| Current address: Anorganish-Chemisches Institut, Technische Universtiät München, Litchtenbergstr. 4, D-85747 Garching, Germany (Alexander von Humboldt Research Fellow).

(1) Goltner, C. G.; Smarsly, B.; Berton, B.; Antonieitti, M. *Chem. Mater.* **2001**, *13*, 1617.
(2) Liu, Y.; Pinnavaia, T. J. *J. Mater. Chem.* **2002**, *12*, 3179. *J. Am. Chem. Soc.* **2000**, *122*, 8791. Liu, Y.; Zhang, W.; Pinnavaia, T. J. *Angew. Chem., Int. Ed.* **2000**, *40*, 1255.
(3) On, D. T.; Kaliaguine, S. *Angew. Chem., Int. Ed.* **2001**, *40*, 3248; *Angew. Chem., Int. Ed.* **2002**, *41*, 1040.
(4) (a) Zhang, Z. T.; Han, Y.; Zhu, L.; Wang, R. W.; Yu, Y.; Qiu, S. L.; Zhao, D. Y.; Xiao, F. S. *Angew. Chem., Int. Ed.* **2001**, *40*, 1258. (b) Zhang, Z.; Han, Y.; Xiao, F. S.; Qiu, S. L.; Zhu, L.; Wang, R. W.; Yu, Y.; Zhang, Z.; Zou, B. S.; Wang, Y. Q.; Sun, H. P.; Zhao, D. Y.; Wei, Y. *J. Am. Chem. Soc.* **2001**, *123*, 5014. (c) Han, Y.; Wu, S.; Sun, Y.; Li, D.; Xiao, F. S. *Chem. Mater.* **2002**, *14*, 1144. (d) Sun, Y.; Han, Y.; Yuan, L.; Ma, S.; Jiang, D.; Xiao, F. S. *J. Phys. Chem. B* **2003**, *107*, 1853.
(5) (a) Kloetstra, K. R.; Zandbergen, H. W.; Jansen, J. C.; van Bekkum, H. *Chem. Ind. (Dekker)* **1998**, *74*, 159. (b) Kirschhock, C. E. A.; Buschmann, V.; Kremer, S.; Ravishankar, R.; Houssin, C. J. Y.; Mojet, B. L.; van Santen, R. A.; Grobet, P. J.; Jacobs, P. A.; Martens, J. A. *Angew. Chem., Int. Ed.* **2001**, *40*, 2637.
(6) (a) Karlsson, A.; Stöcker, M.; Schmidt, R. *Microporous Mesoporous Mater.* **1999**, *27*, 181. (b) de Moor, P. E. A.; Beelen, T. P. M.; van Santen, R. A.; Tsuji, T.; Davis, M. E. *Chem. Mater.* **1999**, *11*, 36. (c) de Moor, P. E. A.; Beelen, T. P. M.; van Santen, R. A. *J. Phys. Chem. B* **1999**, *103*, 1639. (d) Huang, L.; Guo, W.; Deng, P.; Xue, Z.; Li, Q. *J. Phys. Chem. B* **2000**, *104*, 2817.
(7) (a) Li, Y.; Shi, J.; Chen, H.; Hua, Z.; Zhang, L.; Ruan, M.; Yan, J.; Yan, D. *Microporous Mesoporous Mater.* **2003**, *60*, 51. (b) Li, Y.; Shi, J.; Hua, Z.; Chen, H.; Ruan, M.; Yan, D. *Nano Lett.* **2003**, *3*, 609. (c) Shih, P. C.; Lin, H. P.; Mou, C. Y. *Stud. Surf. Sci. Catal.* **2003**, *146*, 557.
(8) (a) Schmidt, I.; Madsen, C.; Jacobsen, C. J. H. *Inorg. Chem.* **2000**, *39*, 2279. (b) Schmidt, I.; Boisen, A.; Gustavsson, E.; Stahl, K.; Pehrson, S.; Dahl, S.; Carlsson, A.; Jacobsen, C. J. H. *Chem. Mater.* **2001**, *13*, 4416.
(9) Boisen, A.; Schmidt, I.; Carlsson, A.; Dahl, S.; Brorson, M.; Jacobsen, C. J. H. *Chem. Commun.* **2003**, 958.
(10) Tao, Y.; Kanoh, H.; Kaneko, K. *J. Am. Chem. Soc.* **2003**, *125*, 6044; *J. Phys. Chem. B* **2003**, *107*, 10974.

10.1021/cm035293k CCC: $27.50
Published on Web 07/13/2004

colloid imprinted carbon[11] as templates, have also been reported.

Previously, Ryoo and co-workers developed a series of ordered carbon mesoporous molecular sieves (CMK-*n*; $n = 1-5$),[12−15] which possess high surface area and excellent thermal/hydrothermal stabilities. The ordered CMK-1[12] and CMK-3[13,14] materials are prepared by carbonization of mesoporous silicate materials MCM-48[16] or SBA-15,[17] respectively. More recently, several successful attempts in replicating the CMK materials into pure silica forms of SBA-15 and HUM-1[18] under steaming conditions in the presence of HCl have been reported. Nevertheless, despite the fact that these replicated silica materials appear to possess uniform pore size and good surface area, they are not readily applicable for catalytic reactions. Furthermore, mesoporous molecular sieves with amorphous-like walls are known to have lower hydrothermal stability. In the present study, we developed a novel route to synthesize mesoporous molecular sieves with microporous characteristics, namely replicated mesoporous aluminosilicate molecular sieves RMM-1 and RMM-3, which are respectively replicated from carbon mesoporous molecular sieves CMK-1 and CMK-3, using precursors of ZSM-5 zeolite.

Experimental Section

Syntheses of RMM-1 and RMM-3. Mesoporous carbon molecular sieve CMK-1 and CMK-3 was synthesized according to the procedure described elsewhere.[12−14] Further replication of CMK material into mesoporous molecular sieves RMM-1 or RMM-3 was carried by the following steps: (1) ca. 1 g of carbon mesoporous molecular sieve (CMK-1 or CMK-3) was first activated in air at 373 K for 1 h; (2) ca. 10 mL of ethanolic solution containing tetraethyl orthosilicate (TEOS; 5 mL) and a certain amount of aluminum isopropoxide ($Al(ip)_3$; 0.02, 0.04, and 0.06 g for Si/Al = 50, 100, and 150, respectively) were introduced into the activated carbon material; (3) the resultant gel was subjected to aging at 313 K for 48 h to form aluminosilicate/CMK composite; (4) ca. 25 wt % tetrapropylammonium hydroxide (TPAOH; 7 mL) was added before further aging for 1 day at the same temperature; (5) the excess amount of TPAOH was filtered and washed by distilled water then by ethanol; (6) the resultant composite was then allowed to crystallize in the presence of saturated steam at 373 K for 2 d in an autoclave; (7) finally, the as-synthesized CMK/RMM composite (denotes as RMM-1a or RMM-3a) was calcined in air at 873 K for 6 h to obtain a carbon-free sample (denotes as RMM-1c or RMM-3c). Note that unlike most mesoporous materials synthesized via alkali route, it will be shown later that using TPAOH as a hydrolysis agent not only warrants the formation of zeolite secondary building units in the framework but also leads to direct creation of acid sites after calcination. To understand the effect of crystallization time on their formation, samples were allowed to crystallize under steaming (step 6) for different periods of time; they are denoted as RMM-n(*x*)-*y*, where $n = 1$ or 3, x is the crystallization duration (in day) and y represents the Si/Al ratio of the sample. However, for the sake of easy comparison and discussion, only the results obtained from samples respectively synthesized with $x = 2$ d and $y = 100$, i.e., RMM-1(2)-100 and RMM-3(2)-100, are illustrated in this report unless specified otherwise.

Postsynthesis Studies. All RMMs were subjected to standard hydrothermal stability test. This was carried out in an autoclave under autogenously pressure by treating ca. 0.1 g of sample in 20 mL water at 373 K for 1 d. An additional test for mechanical stability was also performed by compressing ca. 0.1 g of RMM sample to 100 MPa for 1 h. The samples after hydrothermal and mechanical treatments are denoted herein as RMM-1h, RMM-3h, RMM-1m, and RMM-3m, respectively.

Characterization Methods. The phase purity of all samples was examined by powdered X-ray diffraction (XRD) with Cu K_α ($\lambda = 0.15418$ nm) radiation. The physical properties (BET surface area, pore size distribution, wall thickness, etc.) of the samples were derived from N_2 adsorption/desorption measurements (at 77 K). Fourier transform-infrared (FT-IR; Bruker IFS-28) spectroscopy was used to identify the vibrational mode of the zeolite secondary building units. Hyperpolarized (HP) ^{129}Xe NMR[19,20] and ^{27}Al MAS NMR experiments were performed on a solid-state 300 MHz (Avance-300, Bruker-Biospin) spectrometer to probe the porosity and the nature of Al coordination of the material. On the other hand, the acid properties of the samples were studied by diffuse reflectance FT-IR spectroscopy (DRIFT) and ^{31}P MAS NMR of the adsorbed trimethylphosphine oxide (TMPO) probe molecule.[21] The latter was performed on a solid-state 500 MHz (MSL-500P; Bruker) spectrometer. Typically, MAS NMR experiments were carried out with sample spinning frequency of 10−12 kHz. Bulk mesoporous materials for TEM characterization were embedded in Spur resin and cured at 333 K overnight. Ultrathin sections (approximately 60−90 nm) were cut from the embedded specimen using a diamond knife. TEM micrographs were taken with a Hitachi H-7100 instrument operated at 75−300 keV. Scanning electron microscopy (SEM) micrographs were taken with a Hitachi S-800 instrument operated at an accelerating voltage of 20 keV.

Results and Discussion

All as-synthesized samples, which originally appeared as black powder, turned into a pure white color after the calcination treatment. The black color of the as-synthesized samples suggests that condensation of aluminosilicates indeed occurred inside the pores of carbon molecular sieves. However, in the case of an excessive amount of TEOS or prolonged aging time the as-synthesized samples become gray in color, revealing the occurrence of silica condensation on the external surface of the mesoporous carbon. An attempt to prepare RMM replicated from CMK by using a nanosized precursor of ZSM-5 results in formation of zeolite nanocrystals on the external surface of the carbon

(11) Kim, S. S.; Shah, J.; Pinnavaia, T. J. *Chem. Mater.* **2003**, *15*, 1664.
(12) Ryoo, R.; Joo, S. H.; Jun, S. *J. Phys. Chem. B* **1999**, *103*, 7743.
(13) Jun, S.; Joo, S. H.; Ryoo, R.; Kruk, M.; Jaroniec, M.; Liu, Z.; Ohsuna, T.; Terasaki, O. *J. Am. Chem. Soc.* **2000**, *122*, 10712.
(14) Ryoo, R.; Joo, S. H.; Kruk, M.; Jaroniec, M. *Adv. Mater.* **2001**, *13*, 677.
(15) (a) Joo, S. H.; Chol, S. J.; Oh, I.; Kwak, J.; Liu, Z.; Terasaki, O.; Ryoo, R. *Nature* **2001**, *412*, 169. (b) Ryoo, R.; Joo, S. H.; Jun, S.; Tsubakiyama, T.; Terasaki, O. *Stud. Surf. Sci. Catal.* **2001**, *135*, 150.
(16) (a) Beck, J. S.; Vartuli, J. C.; Roth, W. J.; Leonowicz, M. E.; Kresge, C. T.; Schmitt, K. D.; Chu, C. T. W.; Olson, D. H.; Sheppard, E. W.; McCullen, S. B.; Higgins, J. B.; Schlenker, J. L. *J. Am. Chem. Soc.* **1992**, *114*, 10834. (b) Kresge, C. T., Leonowicz, M. E.; Roth, W. J.; Vartuli, J. C.; Beck, J. S. *Nature* **1992**, *359*, 710.
(17) (a) Zhao, D.; Feng, J.; Huo, Q.; Melosh, N.; Fredrickson, G. H.; Chmelka, B. F.; Stucky, G. D. *Science* **1998**, *279*, 548. (b) Zhao, D.; Huo, Q.; Feng, J.; Chmelka, B. F.; Stucky, G. D. *J. Am. Chem. Soc.* **1998**, *120*, 6024.
(18) (a) Kang, M.; Yi, S. H.; Lee, H. I.; Yie, J. E.; Kim, J. M. *Chem. Commun.* **2002**, 1944. (b) Lu, A. H.; Schmidt, W.; Taguchi, A.; Spliethoff, B.; Tesche, B.; Schüth, F. *Angew. Chem., Int. Ed.* **2002**, *41*, 3489. (c) Kim, J. Y.; Yoon, S. B.; Yu, J. S. *Chem. Mater.* **2003**, *15*, 1932.
(19) Raffery, M. D.; Chmelka, B. F. In *NMR Basic Principles and Progress;* Bluemich, B., Kosfeld, R., Eds.; Springer-Verlag: Berlin, 1993; Vol. 30, p 111.
(20) Moudrakovski, I. L.; Terskikh, V. V.; Ratcliffe, C. I.; Ripmeester, J. A.; Wang, L. Q.; Shin, Y.; Exarhos, G. J. *J. Phys. Chem. B* **2002**, *106*, 5938.
(21) Zhao, Q.; Chen, W. H.; Huang, S. J.; Wu, Y. C.; Lee, H. K.; Liu, S. B. *J. Phys. Chem. B* **2002**, *106*, 4462, and references therein.

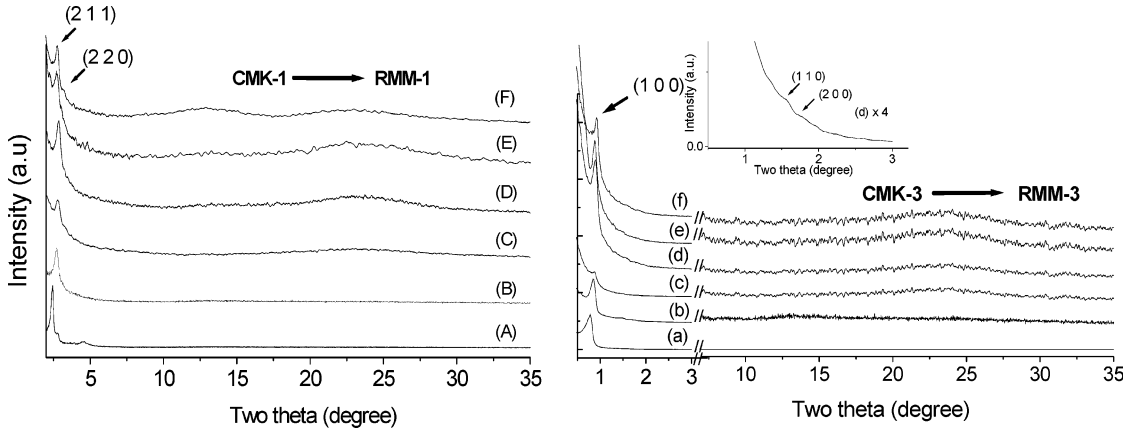

Figure 1. XRD patterns of (A, a) MCM-48, SBA-15; (B, b) CMK-1, CMK-3; (C, c) RMM-1a, RMM-3a; (D, d) RMM-1c, RMM-3c; (E, e) RMM-1m, RMM-3m; and (F, f) RMM-1h, RMM-3h.

template. In this case, the final product also appeared as gray color. Alternatively, RMMs can also be synthesized by first treating the mesoporous carbon by TPAOH and then introduction of aluminosilicates followed by crystallization. Nevertheless, the RMMs so prepared are somewhat less ordered and reveal poor crystallinities than the materials prepared by the aforementioned procedures (see Experimental Section). In any case, the methodology report here thus is more favorable for introducing aluminosilicates in the confined space of carbon molecular sieves.

Figure 1 displays the XRD profiles of various samples. The as-synthesized RMM/CMK composite materials, namely RMM-1a and RMM-3a, both exhibit a weak diffraction peak at a respective 2θ angle of ca. 2° (Figure 1C) and 0.8° (Figure 1c), revealing typical characteristics of a mesoporous structure similar to that of CMK-1 (Figure 1B) and CMK-3 (Figure 1b), which are carbon replicas of MCM-48 (Figure 1A) and SBA-15 (Figure 1a), respectively. The above observation indicates that most of the mesoporous voids of carbon molecular sieves were filled with aluminosilicate composites. Figure 1D,d shows the respective XRD patterns of RMM-1c and RMM-3c samples after the removal of their corresponding carbon template by calcination treatment. The mesoporous characteristics of these target materials are also evident. In particular, the XRD pattern of the RMM-1c sample shows a main [211] peak with a weak shoulder [220], whereas that of the RMM-3c sample exhibits a main peak [100] along with weak shoulder peaks corresponding to [110] and [200] (see insert in Figure 1). That no additional peaks are visible at a higher diffraction angle ($2\theta \geq 8°$) in as-synthesized nor calcined RMMs indicates the absence of any isolated microporous zeolite crystallites within the detection limit of the XRD apparatus (ca. 5 nm in size).[22] Successful replications of CMKs into RMMs through this novel method can thus be inferred. That the XRD patterns of the calcined RMM samples remain intact after mechanical (i.e., samples RMM-1m and RMM-3m; see Figure 1E,e) and hydrothermal (RMM-1h and RMM-3h; Figure 1F,f) stability tests confirms that the RMMs possess high mechanical and hydrothermal stabilities. An additional steam stability test also indicates that these novel RMMs retain their structure even under steaming at 773 K for 6 h. This is a priori due to the presence of zeolitic secondary building units in the structural frameworks of the RMMs, as will be discussed below.

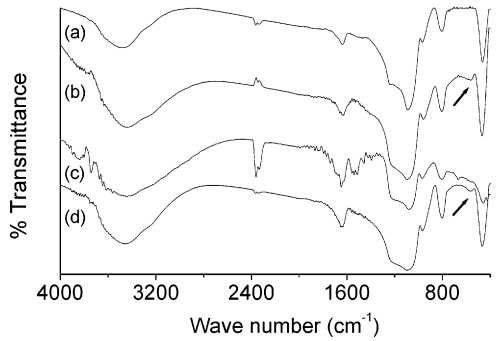

Figure 2. FT-IR spectra of (a) Al-MCM-48, (b) RMM-1c, (c) SBA-15, and (d) RMM-3c.

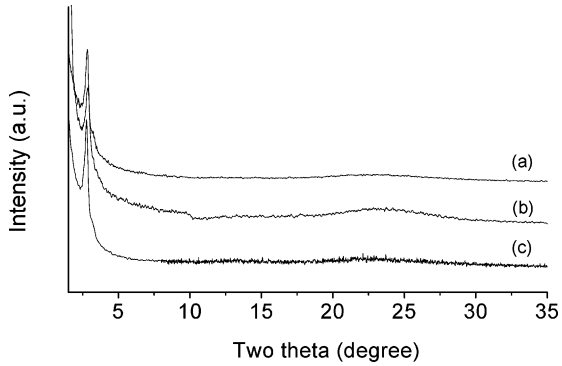

Figure 3. XRD patterns of RMM-1c samples synthesized with steaming period of 2 d and Si/Al ratios of (a) 50, (b) 100, and (c) 150.

Figure 2 displays the FT-IR spectra of calcined Al-MCM-48 (Si/Al = 100), RMM-1c, SBA-15, and RMM-3c samples. While the spectra obtained from these samples all reveal characteristics of mesoporous silicate/aluminosilicate framework, an additional weak broad band near 540 cm^{-1} was observed for RMM-1c and RMM-3c samples, as shown in Figure 2 (parts b and d, respectively). This peak, which is invisible in both Al-MCM-48 and SBA-15, is commonly ascribed to the existence of zeolite secondary building units in the framework.[22] Similar observation was also found in other mesoporous materials synthesized using a zeolite precursor under hydrothermal conditions.[5] In this context, the use of

(22) On, D. T.; Kaliaguine, S. *J. Am. Chem. Soc.* **2003**, *125*, 618.

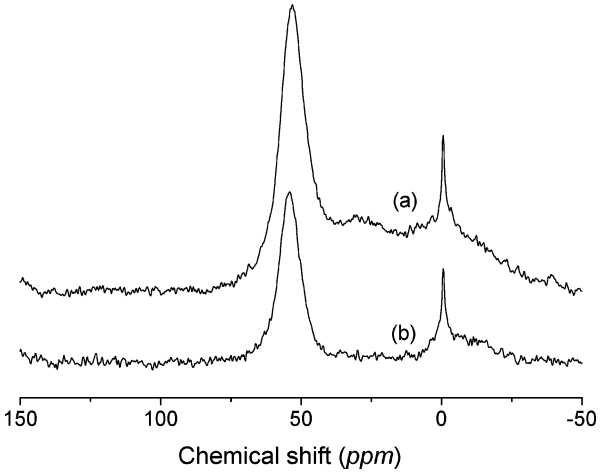

Figure 4. Room temperature ^{27}Al MAS NMR spectra of hydrated (a) RMM-1c and (b) RMM-3c.

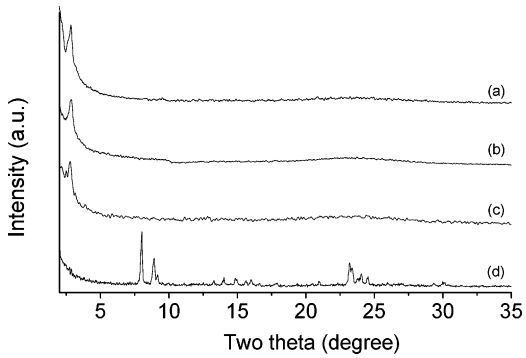

Figure 5. XRD patterns of RMM-1c samples (Si/Al = 100) synthesized with different steaming periods of (a) 1 d, (b) 2 d, (c) 3 d, and (d) 5 d.

TPAOH as a hydrolyzing agent thus favors the formation of zeolite secondary building units in the framework of RMMs.

Figure 3 displays the XRD patterns of RMM-1c samples synthesized with different Si/Al ratios. It is indicative that the structures of RMMs remain practically unchanged even in the presence of a wide range of Al in the framework. Further experiments by ^{27}Al MAS NMR indicate that the majority of the Al species in the hydrated RMMs are tetrahedral coordinated Al, resulting in a strong broad peak at ca. 52 ppm (Figure 4). However, it is also found that the amount of extraframework (octahedral coordinated) Al tends to increase with an increasing Al content (not shown). In this context, the novel synthesis route report here is more favorable for preparing RMMs with Si/Al $\geq$ 100.

To explore the effect of steaming on structural and physical properties of RMMS, samples with the same Si/Al = 100 but subjected to different seaming periods were examined. As an illustration, the XRD patterns and FT-IR spectra of RMM-1c samples prepared by varying the steaming period from 1 to 5 d are shown in Figures 5 and 6, respectively. A consistent decrease in the crystallinity of mesoporous phase with an increasing steaming period can be evidenced by the decrease in [211] peak intensity of the XRD patterns from Figure 5a−c. As the steaming period exceeds 5 d, the XRD pattern reveals only characteristics of the ZSM-5 structure (Figure 5d), indicating that the prolonged steaming treatment tends to provoke silica condensation on the

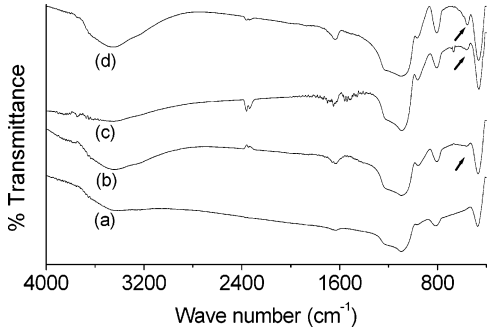

Figure 6. FT-IR spectra of RMM-1c samples (Si/Al =100) synthesized with different steaming periods of (a) 1 d, (b) 2 d, (c) 3 d, and (d) 5 d.

exterior of the mesoporous carbon materials resulting in a segregated phase of microcrystalline zeolite. These observations are well reflected in the FT-IR spectra (Figure 6), in which the intensity of the additional band at 540 cm^{-1} reveals the expected increase with an increased steaming period. Results obtained from SEM studies provide supporting evidences. As illustrated in Figure 7a−c for RMM-1c samples, a consistent decrease in uniformity of the resultant product with an increasing steaming period from 1 to 3 days is evident. Further increase in the steaming period however leads to formation of ZSM-5 zeolite crystals, as shown in Figure 7d. Unlike RMM-1 materials, which are less uniform in terms of particle size, the SEM image of RMM-3(2)-100 reveals a more uniform platelike morphology (Figure 7e). This is ascribed due to the larger pore size of CMK-3 (5.4 nm) compare to CMK-1 (2.3 nm). The TEM images of RMM-1c (Figure 8a) and RMM-3c (Figure 8b) further confirm that both materials possess uniform pores with cubic and hexagonal patterns, respectively. The slight disorder observed is most likely due to the incorporation of heteroatoms (i.e., Al) onto the mesoporous silicate frameworks of the replicated materials.[4c]

Nitrogen adsorption/desorption measurements (77 K) on RMMs exhibit the typical type-IV isotherm with a sharp inflection at p/p_0 = 0.45 and 0.65, respectively, for the RMM-1 and RMM-3 samples and a broad hysteresis loop (Figure 9), which is characteristic of capillary condensation in mesoporous channels.[23,24] Accordingly, the BET surface area, pore volume, and pore size (BJH method) of various samples can be derived, and the results are depicted in Table 1. The RMMs possess a typical surface area of 550−600 m^{2}g^{-1}, which is less than that of their parent counterparts, i.e., MCM-48 and SBA-15 (ca. 780−800 m^{2}g^{-1}). In particular, ca. 20−30% of the total surface area in RMMs was found contributed by micropores, which are most likely due to the presence of zeolite secondary building units on their structural framework. Further *t*-plot analyses also confirm the existence of microporosity within the RMMs (Figure 10). Moreover, a total pore volume of 0.8−0.9 cm^{3}g^{-1} (typical for mesoporous structure) is derived for RMMs, in which ca. 10% is provoked by micropores.

(23) Sing, K. S. W.; Everett, D. H.; Haul, R. A. W.; Moscow, L.; Pierotti, R. A.; Rouquerol, T.; Siemienewska, T. *Pure Appl. Chem.* **1985**, *57*, 603.

(24) (a) Kruck, M.; Jaroniec, M. *Chem. Mater.* **2003**, *15*, 1327; *Chem. Mater.* **2001**, *13*, 3169. (b) Ravikovitch, P. I.; Neimark, A. V. *Langmuir* **2002**, *18*, 1550. (c) Liu, H.; Zhang, L.; Seaton, N. A. *J. Colloid Interface Sci.* **1993**, *156*, 285. (d) Ball, P. C.; Evans, R. *Langmuir* **1989**, *5*, 714.

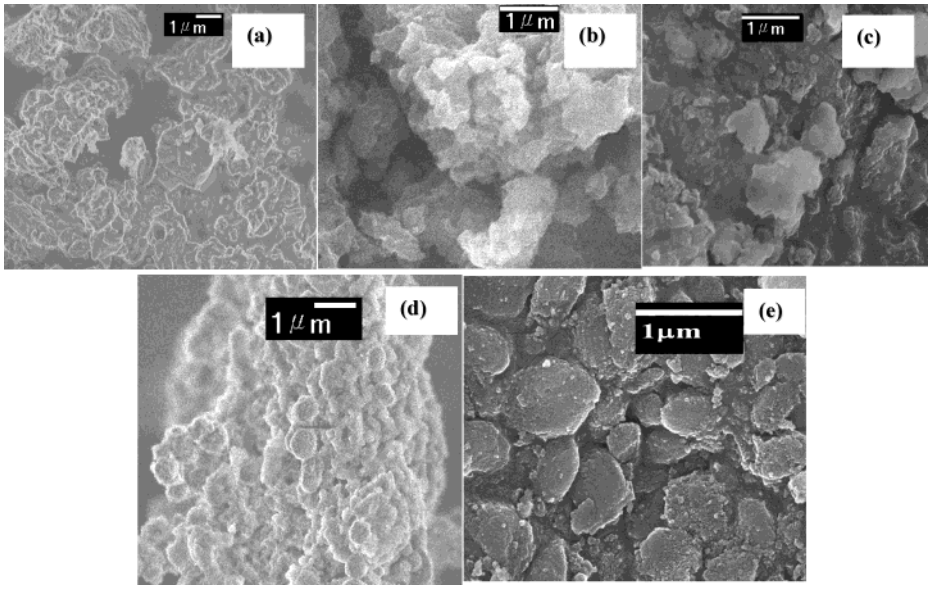

Figure 7. SEM pictures of RMM-1c (Si/Al = 100) synthesized with different steaming periods of (a) 1 d, (b) 2 d, (c) 3 d, and (d) 5 d. The SEM picture of (e) RMM-3(2)-100 is also shown for comparison.

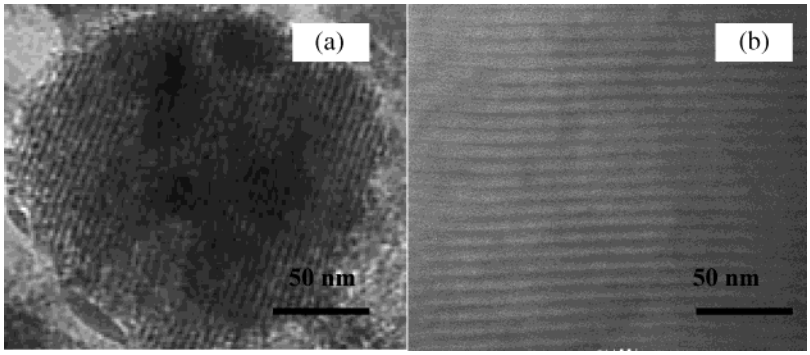

Figure 8. TEM images of (a) RMM-1c and (b) RMM-3c.

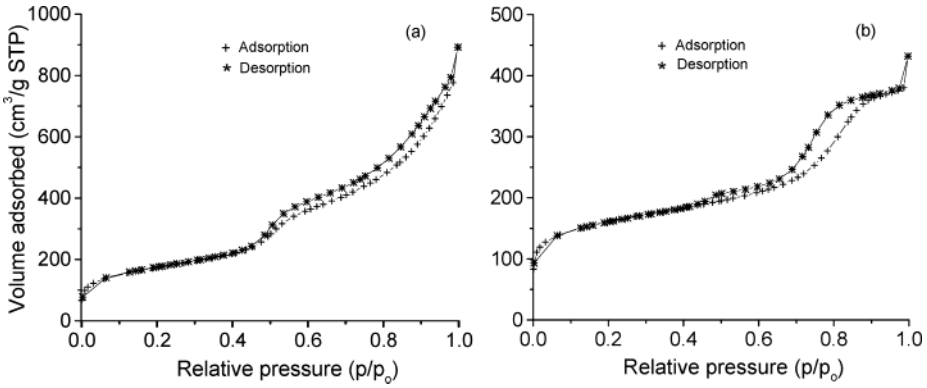

Figure 9. N_2 adsorption/desorption curves of (a) RMM-1c and (b) RMM-3c.

Table 1. Physical Properties of Various Samples Obtained from N_2 Adsorption/Desorption Measurements at 77 K

sample	BET_{total} ($m^2\,g^{-1}$)	BET_{micro}[a] ($m^2\,g^{-1}$)	BET_{micro}/BET_{total} (%)	V_{total} ($cm^3\,g^{-1}$)	V_{micro} ($cm^3\,g^{-1}$)	d_{meso} (nm)
MCM-48	1043			0.78		2.5−2.8
RMM-1c	554	154	27.8	0.77	0.07	3−5
SBA-15	796	230	28.8	0.73	0.07	5−7
RMM-3c	595	178	29.9	0.92	0.08	4−6

[a] Microporous surface area calculated using *t*-plot analysis.

Analyses by the BJH method reveal that both RMM-1 and RMM-3 have a broad distribution of pore size centered at 3.3 and 5.7 nm, respectively. The effects of the steaming period and the Al content on physical properties are illustrated by various RMM-1 samples in Table 2. It is conclusive that while prolonged steaming results in a consistent decrease in total BET surface area, the surface area responsible for microporosity and

Table 2. Physical Properties Obtained from N_2 Adsorption/Desorption Measurements at 77 K for RMM-1 Samples Synthesized with Different Steaming Periods and Si/Al Ratios

sample	BET_{total} (m^2g^{-1})	BET_{micro}[a] (m^2g^{-1})	BET_{micro}/BET_{total} (%)	V_{total} (cm^3g^{-1})	V_{micro} (cm^3g^{-1})	d_{meso} (nm)
RMM-1(1)-100	628	147	23.4	0.68	0.06	3−5
RMM-1(2)-100	554	154	27.8	0.77	0.07	3−5
RMM-1(3)-100	422	146	34.6	0.36	0.07	3−5
RMM-1(2)-150	632	82	13.0	0.93	0.04	4−6
RMM-1(2)-50	638	66	10.4	0.89	0.03	4−5

[a] Microporous surface area calculated using *t*-plot analysis.

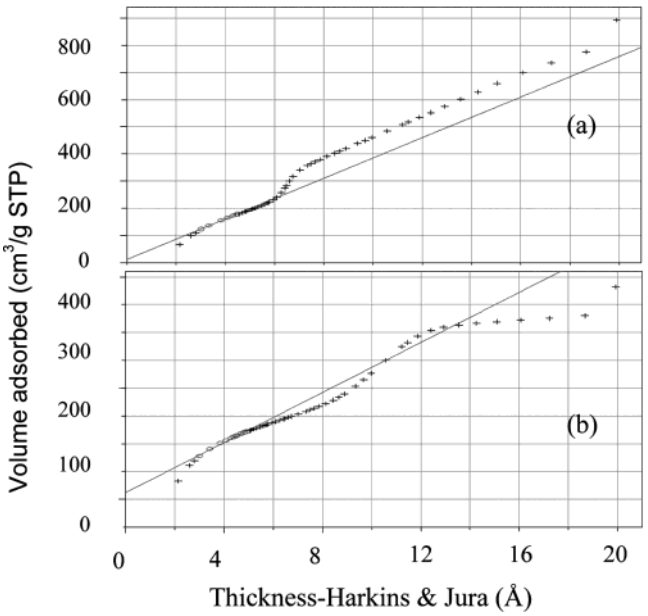

Figure 10. The *t*-plots obtained from N_2 adsorption/desorption measurements of (a) RMM-1c and (b) RMM-3c.

the pore size remain practically unchanged. In terms of Al content, a sample prepared with Si/Al = 100 seems to be more favorable for formation of microporosity compared to a sample with Si/Al = 150. This may be due to the presence of more tetrahedral coordinated Al species on the structural framework of the former sample. However, as evidenced by ^{27}Al MAS NMR, a further increase in Al content tends to provoke formation of extraframework Al species, thus resulting in an overall decrease in microporosity. The above results obtained from N_2 adsorption/desorption measurements are therefore consistent with the XRD, SEM, FT-IR, and ^{27}Al MAS NMR results discussed earlier.

The porosity of RMMs was further characterized by continuous flow, hyperpolarized (HP) ^{129}Xe NMR technique.[19,20] Unlike the conventional ^{129}Xe NMR method by which the ^{129}Xe chemical shifts are largely dictated by the Xe−Xe interactions, HP ^{129}Xe NMR can be accomplished at dilute Xe loading, and hence the observed chemical shifts reflect interactions between the Xe atom and the inner surface of the porous adsorbent.[20] Accordingly, different porous environments can be inferred from the variations of the ^{129}Xe chemical shift with temperature, as shown in Figure 11. The HP ^{129}Xe NMR spectra of Xe (partial pressure 15.6 Torr) adsorbed on dehydrated RMMs at room temperature reveals a broad, asymmetric resonance in the downfield direction

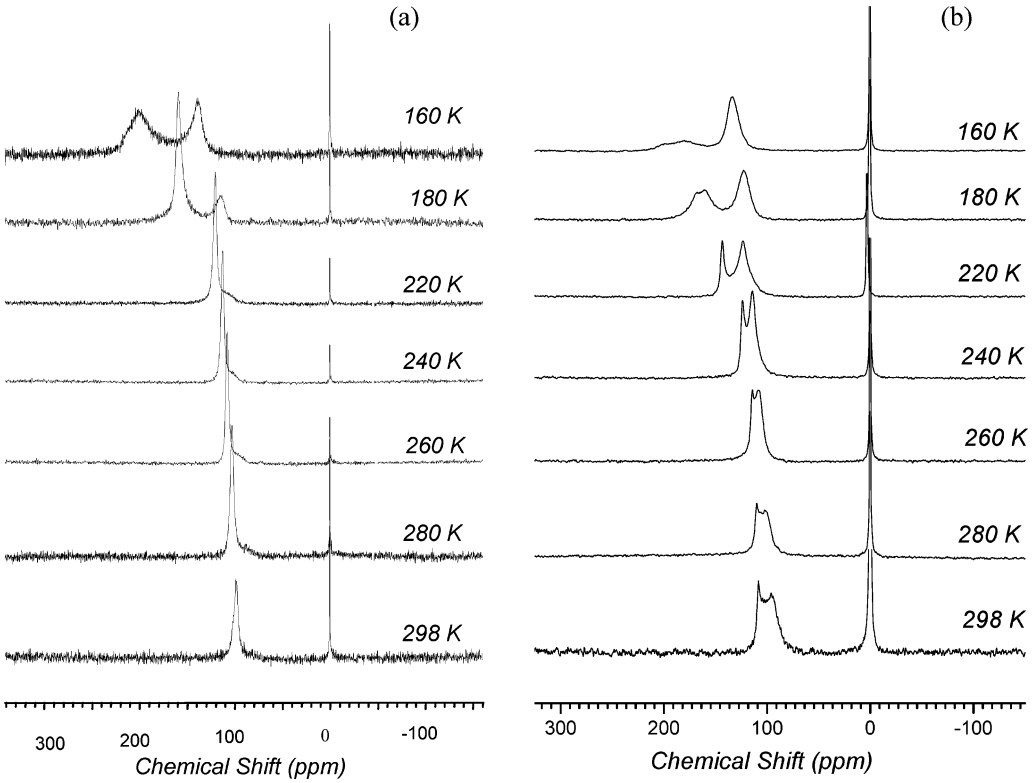

Figure 11. Variable temperature HP ^{129}Xe NMR spectra of Xe (partial pressure 15.6 Torr) adsorbed on (a) RMM-1c and (b) RMM-3c.

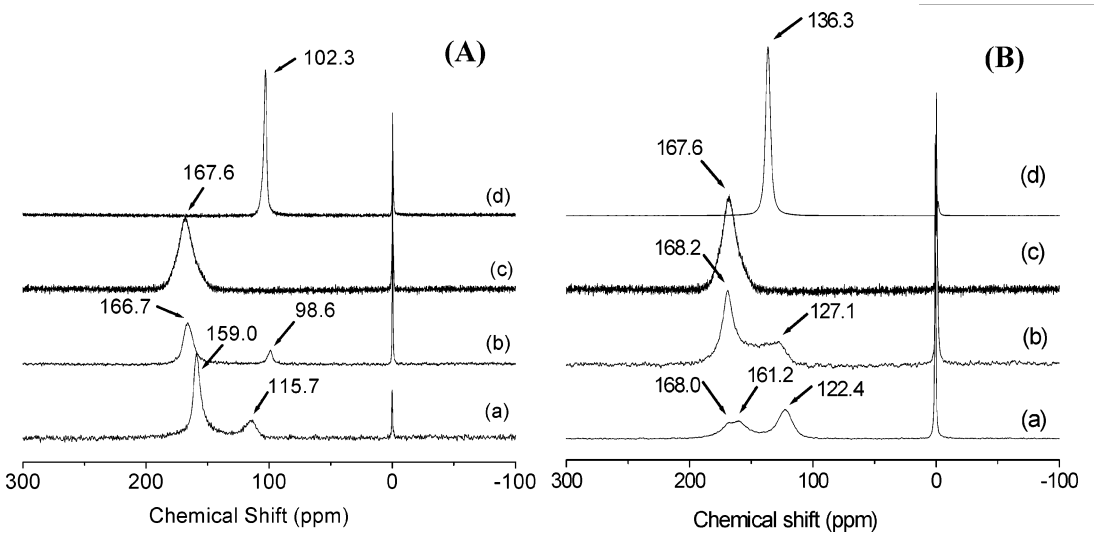

Figure 12. HP ^{129}Xe NMR spectra of Xe adsorbed on various samples at 180 K; (A-a) RMM-1c, (A-b) 1:1 physical mixture of Al-MCM-48 (Si/Al = 100) and ZSM-5 (Si/Al = 140), (A-c) ZSM-5, (A-d) Al-MCM-48, (B-a) RMM-3c, (B-b) 1:1 physical mixture of SBA-15 (Si/Al = 100) and ZSM-5 (Si/Al = 140), (B-c) ZSM-5, and (B-d) SBA-15.

relative to the reference (i.e. dilute gaseous Xe) peak at 0 ppm. Upon decreasing temperature, the observed chemical shifts increase due to the slight increase in Xe loading. Further decreasing the temperature below 180 K, the resonance eventually splits into a doublet and a triplet for RMM-1c (Figure 11a) and RMM-3c (Figure 11b), respectively, indicating the presence of different pore distribution environments in the replicated materials. Specifically, for RMM-1c, the spectrum at 180 K exhibits two distinct peaks at 159.0 and 115.7 ppm, which can be assigned due to Xe adsorbed in a microporous zeolite secondary building unit and mesopores, respectively. The HP ^{129}Xe NMR spectra of ZSM-5 (Si/Al = 140), Al-MCM-48 (Si/Al = 100), and the 1:1 physical mixture of the ZSM-5 and Al-MCM-48 obtained at 180 K are shown in Figure 12A for comparison. It is clear that while both microporous ZSM-5 zeolite (Figure 12A-c) and mesoporous Al-MCM-48 molecular sieve (Figure 12A-d) show only a single resonance peak at 180 K revealing a uniform pore distribution, two distinct peaks at 166.7 and 98.6 ppm are evident for the 1:1 physical mixture sample (Figure 12A-b). This suggests that at the given NMR time-scale, a fast exchange of Xe between two types of pores exist at low-temperature analogous to that of RMM-1c (Figure 12A-a). The chemical shift difference between the two major peaks in RMM-1c being smaller than that in the physical mixture sample provides additional support to the presence of a microporous zeolite secondary building unit on the mesoporous RMM-1.[6d] A similar observation can be found for RMM-3, except that in this case, three resonance at 168.0, 161.2, and 122.4 ppm can be resolved (Figure 12B-a). By comparison, the spectrum obtained from SBA-15 shows only a singlet at 136.4 ppm (Figure 12B-d), whereas the 1:1 SBA-15 and ZSM-5 physical mixture sample exhibits a broad resonance spanning from 168.2 to 127.1 ppm (Figure 12B-b). Since SBA-15 is known to possess mesopores as well as microporous warm holes, it is hypothesized that the three distinct resonances at 168.0, 161.2, and 122.4 ppm observed for RMM-3 at low temperature are due to Xe adsorbed in a microporous zeolite secondary building unit, microporous warm holes, and mesopores, respectively.

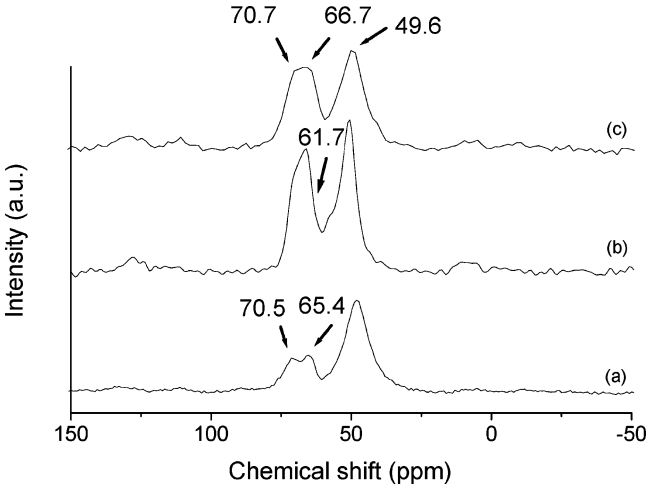

Figure 13. ^{31}P MAS NMR spectra of TMPO adsorbed on various samples with Si/Al = 100: (a) Al-MCM-48, (b) RMM-1c, and (c) RMM-3c.

In terms of acidity of RMMs, the DRIFT spectra of RMM-1c and RMM-3c samples reveal a broader distribution of Brønsted acidity (at ca. 3650 cm^{-1}; not shown) compared to Al-MCM-48, especially for a sample after hydrothermal treatment. Separate experiments using ^{31}P MAS NMR of trimethylphosphine oxide (TMPO) probe molecule[21] adsorbed on RMMs confirms the existence of Brønsted acid sites in the samples. As shown in Figure 13, the ^{31}P NMR spectra of TMPO adsorbed on Al-MCM-48, RMM-1c, and RMM-3c samples with Si/Al = 100 all exhibit similar multiple resonance. Detailed spectral simulation by Gaussian deconvolution[21] further revealed that four distinct resonances at 70.5, 65.4, 61.2, and 49.6 (± 1) ppm can be resolved. While the peak at 49.6 ppm can be unambiguously assigned due to physisorbed TMPO, the other three resonance are due to TMPO interacting with Brønsted acid sites. The higher the observed ^{31}P chemical shift the higher the acidic strength of the acid sites.[21] By comparing the relative peak intensities of the resonance in Figure 13a,b, it is clear that while the acid strengths (or chemical shifts)

for each type of Brønsted acidity remain practically unchanged, the novel replicated material (RMM-1c) indeed possesses a higher acid concentration compared to Al-MCM-48 with the same Si/Al ratio. A similar conclusion can be drawn for the RMM-3c vs SBA-15 sample. Additional experiments by TGA also confirmed that the novel RMM-1c is more hydrophilic in nature compared to its parent counterpart, namely Al-MCM-48.

Summary and Conclusions

In conclusion, a novel route for preparing aluminosilicate mesoporous materials with zeolite secondary building unit has been developed. These novel RMMs, which were replicated from carbon mesoporous molecular sieves using zeolite precursors, are found to possess desirable acidity and high hydrothermal, mechanical and steam stabilities.

Acknowledgment. The support of this work by National Science Council, R.O.C. (NSC92-2113-M-001-049 to S.B.L.) is gratefully acknowledged. The authors thank Profs. C. Y. Mou and S. Cheng (National Taiwan University, Taiwan) for helpful discussions.

CM035293K